

ACCURATE 3D MEASUREMENT FROM TWO SAR IMAGES WITHOUT PRIOR KNOWLEDGE OF SCENE

Karl Insfran, Koichi Ito, and Takafumi Aoki

Graduate School of Information Sciences, Tohoku University,
6-6-05, Aramaki Aza Aoba, Sendai, 980-8579, Japan.
E-mail: karl@aoki.ecei.tohoku.ac.jp

ABSTRACT

Remote sensing using Synthetic Aperture Radar (SAR) is an indispensable technology for effective disaster management, owing to its large observation area, cloud penetrating ability and its independence from sunlight, which allow for quick observation of large disaster affected areas disregarding weather or time of the day. In particular, 3D measurement from SAR images could contribute a better understanding of the affected area and speed up decision making. Most methods require prior knowledge of the scene such as ground control points to achieve a reasonable level of 3D measurement accuracy, resulting in losing the advantage of quick observation. In this paper, we propose an accurate 3D measurement method from SAR images based on the principle of stereo vision without any prior knowledge of the scene. We demonstrate the effectiveness of our method compared with the conventional method through a set of experiments using an airborne SAR image dataset.

Index Terms— SAR, radargrammetry, stereo vision, Earth ellipsoid

1. INTRODUCTION

Remote sensing is a technology using sensors mounted on satellites or aircraft to acquire information about a specific ground surface without physical contact [1]. It has been widely used not only in observing the vegetation, temperature, and terrain of the Earth, but also in observing areas affected by natural disasters such as earthquakes, tsunamis, and volcanic eruptions [2]. One of the fundamental and most important techniques in remote sensing is 3D measurement. For example, during a natural disaster, 3D measurement of the affected area is necessary for understanding the situation of the affected area, assessing the damage, reducing the effects of the disaster, and planning rescue operations. Other applications of 3D measurement using remote sensing include canopy structure analysis [3, 4], urban DEM generation [5], and 3D measurement of mountains such as Mt. Fuji [6]. One of the most widely used radars in remote sensing is the Synthetic Aperture Radar (SAR). SAR is an imaging radar using antennas mounted on a moving platform such as a satellite or an airplane to scan the surface of the Earth by emitting radio waves and receiving their reflected waves. Apart from common radar properties such as independence from weather or time of the day, SAR uses pulse compression and aperture synthesis to achieve extremely high spatial resolution. In this paper, we focus on 3D measurement of the target area by utilizing the features of SAR as described above.

There are two approaches to 3D measurement from two SAR images: Cross-track Interferometric SAR (InSAR) [7] and radargrammetry [8]. InSAR measures the height of the target area from

the phase difference between two SAR images by solving phase discontinuity using phase unwrapping. Although the measurement accuracy of InSAR is high, InSAR needs two SAR images of the same area with only slightly different angles, limiting the flight path for SAR image acquisition, and ground control points are indispensable in phase unwrapping in order to obtain absolute elevation values. Radargrammetry measures the height of the target area by using the correspondence between two SAR images of the same area taken on different flight paths. Compared to InSAR, radargrammetry can measure absolute height, but with lower accuracy [8]. In our previous work, we proposed a 3D measurement method from two SAR images based on the principle of stereo vision [9]. We have achieved a high measurement accuracy comparable to InSAR by defining internal and external parameters and the SAR projection model for stereo vision, and introducing parameter optimization based on the minimization of the reprojection error. This method has three problems: (i) parameter optimization is highly dependent on the terrain characteristics, (ii) it assumes that the Earth is flat, and (iii) it requires additional information such as the average height of the scene.

Addressing these problems and improving the accuracy of 3D measurement, we propose a 3D measurement method from SAR images without any prior knowledge of the scene. We define a new SAR projection model that takes the Earth ellipsoid into account, and propose a parameter optimization method that is not affected by the terrain characteristics. We demonstrate the effectiveness of the proposed method through experiments using airborne SAR images taken near Mt. Aso, Kumamoto, Japan.

2. 3D MEASUREMENT USING SAR IMAGES

This section presents our 3D measurement method from SAR images that takes into account the model of the Earth ellipsoid. First, we define the internal parameters required for the SAR projection model and the external parameters that represent the relative position of the antenna between the two images. Next, we define new external parameters that take into account the Earth ellipsoid and derive the theoretical formulas required to calculate the 3D coordinates.

2.1. SAR Projection Model

The SAR projection model is defined by the relation between the position of the target in 3D space and that in 2D space in the SAR image. We employ the digital image coordinate system for the 2D coordinate system as shown in Fig. 1 (a), where the u axis corresponds to the azimuth direction, the direction in which the airplane moves, while the v axis corresponds to the range direction, direction in which the antenna scans the surface. We also employ the radar

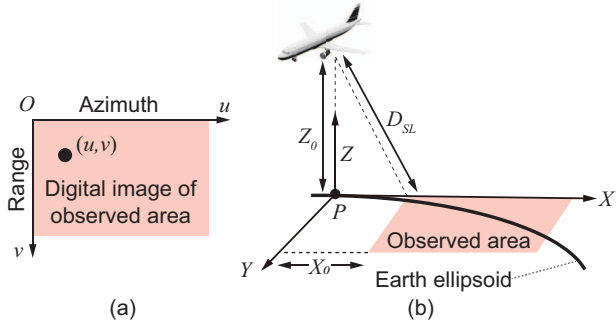


Fig. 1. Digital image coordinate system (a) and radar coordinate system (b).

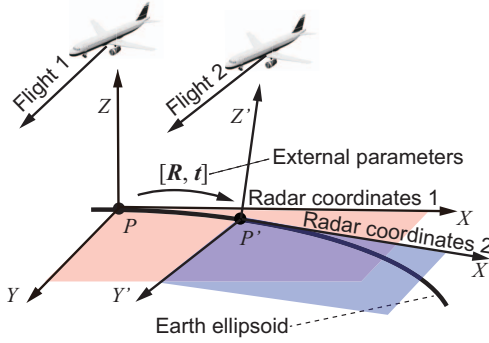


Fig. 2. External parameters \mathbf{R} and \mathbf{t}

coordinate system for the 3D coordinate system as shown in Fig. 1 (b). The radar coordinate system is defined based on a point P on the Earth ellipsoid just below the antenna. We define the X -axis direction as the range direction, the Y -axis direction as the azimuth direction, and the Z -axis direction as normal to the Earth ellipsoid at point P . Note that the position of P can be easily calculated from the latitude and longitude of the airplane and the Earth ellipsoid model. The relation between the radar coordinate system (X, Y, Z) and the digital image coordinate system (u, v) is given by

$$u = \alpha_u Y, \quad (1)$$

$$v = \alpha_v \left(\sqrt{(X_0 + X)^2 + (Z_0 - Z)^2} - D_{SL} \right), \quad (2)$$

where X_0 is the horizontal distance from the antenna to the target corresponding to the SAR image origin, D_{SL} is the linear distance to the SAR image origin, and Z_0 is the height from P to the antenna. α_u and α_v are the inverse of the SAR image resolution along the azimuth and range directions, respectively. X_0 is calculated from Z_0 and D_{SL} using the Pythagorean theorem. We define α_u , α_v , Z_0 , and D_{SL} as the internal parameters of the SAR projection model, which are obtained from the metadata during SAR image acquisition.

2.2. External Parameters Based on Earth Ellipsoid

In our previous work [9], the Earth was assumed to be flat and both radar coordinates in Fig. 2 were approximated to have parallel Z -axes, resulting in large measurement errors depending on the observation conditions. In our method proposed in this paper, we define

the external parameters of SAR taking into account that the Earth is an ellipsoid to improve the accuracy of 3D measurement. Let P and P' be the points on the Earth ellipsoid directly below each SAR antenna, respectively, and (X, Y, Z) and (X', Y', Z') be the radar coordinate system with origin P and P' for each SAR antenna, respectively, as shown in Fig. 2. The relation between both radar coordinate systems can be written by

$$\begin{bmatrix} X' \\ Y' \\ Z' \end{bmatrix} = \mathbf{R} \begin{bmatrix} X \\ Y \\ Z \end{bmatrix} + \mathbf{t}, \quad (3)$$

where \mathbf{R} and \mathbf{t} are a 3×3 rotation matrix and a translation vector, respectively, which are given by

$$\mathbf{R} = \begin{bmatrix} R_{11} & R_{12} & R_{13} \\ R_{21} & R_{22} & R_{23} \\ R_{31} & R_{32} & R_{33} \end{bmatrix}, \quad \mathbf{t} = \begin{bmatrix} t_X \\ t_Y \\ t_Z \end{bmatrix}. \quad (4)$$

We define (\mathbf{R}, \mathbf{t}) as the external parameters of SAR.

2.3. Theoretical Formula for 3D Measurement

If the correspondence between two SAR images can be obtained, the 3D coordinates of the target can be calculated using the SAR projection model and the relation between radar coordinate systems. Let (u, v) and (u', v') represent the 2D coordinates of SAR image 1 and 2, respectively. (u, v) and (u', v') are given by

$$u = \alpha_u Y, \quad (5)$$

$$v = \alpha_v \left(\sqrt{(X_0 + X)^2 + (Z_0 - Z)^2} - D_{SL} \right), \quad (6)$$

$$u' = \alpha'_u (X R_{21} + Y R_{22} + Z R_{23} + t_Y), \quad (7)$$

$$v' = \alpha'_v \left\{ \left((X'_0 + X R_{11} + Y R_{12} + Z R_{13} + t_X)^2 + (Z'_0 - X R_{31} - Y R_{32} - Z R_{33} - t_Z)^2 \right)^{\frac{1}{2}} - D'_{SL} \right\}. \quad (8)$$

By selecting three out of the four equations and solving them as simultaneous equations, we can analytically obtain 3D coordinates. For example, if Eq. (5)–(7) are selected, (X, Y, Z) is derived as

$$X = \sqrt{\left(\frac{v}{\alpha_v} + D_{SL} \right)^2 - (Z_0 - Z)^2} - X_0, \quad (9)$$

$$Y = \frac{u}{\alpha_u}, \quad (10)$$

$$Z = \frac{-b \pm \sqrt{b^2 - 4ac}}{2a}, \quad (11)$$

where a , b , c , and d used in c are given by

$$a = R_{33}^2 + R_{21}^2, \quad (12)$$

$$b = -2(R_{33}d + R_{21}^2 Z_0), \quad (13)$$

$$c = d^2 + R_{21}^2 Z_0^2 - R_{21}^2 \left(\frac{u}{\alpha_u} + D_{SL} \right)^2, \quad (14)$$

$$d = \frac{u'}{\alpha'_u} - \frac{u}{\alpha_u} R_{22} - t_Y + R_{21} X_0. \quad (15)$$

2.4. 3D Measurement Algorithm

The 3D measurement algorithm proposed in this paper consists of (i) parameter setting, (ii) ground projection, (iii) image correspondence, (iv) external parameter optimization, and (v) 3D measurement. The details of each step are described below.

(i) Parameter Setting: The first step is to set the SAR internal and external parameters. The internal parameters are obtained from the metadata of the SAR image acquisition. The external parameters are calculated from the two antenna positions, the flight direction, and the Earth ellipsoid model.

(ii) Ground Projection: Ground projection is an important process for image correspondence to suppress the deformation between SAR images. The SAR image can be projected onto the $X - Y$ plane using Eq. (1) and (2), however this process requires the height Z of each pixel. Most methods employ the average height of the scene taken from the metadata to perform the ground projection. The proposed method performs ground projection without requiring any prior knowledge of the scene. We perform rough image correspondence matching between SAR images projected onto the $X - Y$ plane using Z , which is in the range of 0–4000m with 500m increments. Note that we use the same image correspondence matching method as in the next step. We select the Z with the highest matching score as the average height for ground projection and perform corresponding matching for all pixels.

(iii) Image Correspondence: We employ an image correspondence method using Phase-Only Correlation (POC) [10] since its effectiveness in SAR image processing has been previously demonstrated [9, 11, 12, 13, 14]. POC is an image matching technique that uses phase information obtained by Discrete Fourier Transform of the given images [15]. The correspondence matching method using POC employs (i) a coarse-to-fine strategy using image pyramids for robust correspondence search and (ii) a sub-pixel translational displacement estimation method using POC for local block matching [10].

(iv) External Parameter Optimization: The external parameters defined by Eq. (4) contain a small amount of error since they are obtained from the flight information measured by GPS. We optimize the external parameters by minimizing the reprojection error in the same way as in stereo vision. Only corresponding points with high matching scores are selected to reduce the effect of outliers. We divide the SAR image into m regions and extract n points with the highest matching score from each region since the corresponding points may be locally concentrated, where $m = 25$ and $n = 30$ in this paper. RANSAC [16] is used to simultaneously minimize the reprojection error and further remove outliers. Finally, the parameters that give the lowest reprojection error and have more than a minimum number of inliers are selected.

(v) 3D Measurement: The 3D coordinate (X, Y, Z) for each pixel in the reference image is calculated using the internal and external parameters obtained in steps (i) and (iv), the correspondence obtained in step (ii), and Eqs. (9)–(11)).

3. EXPERIMENTS AND DISCUSSION

This section describes the performance evaluation of the proposed method through experiments using airborne SAR images. In the experiments, we use SAR amplitude images taken by the airborne X-band SAR system developed by National Institute of Information and Communications Technology (NICT), Japan [17]. There are 3 image pairs (Aso A, B, and C) taken near Mt. Aso, Kumamoto, Japan. Fig. 3 shows the image pairs of Aso A, B, and C. We perform 3D measurement of the ground surface from two SAR amplitude

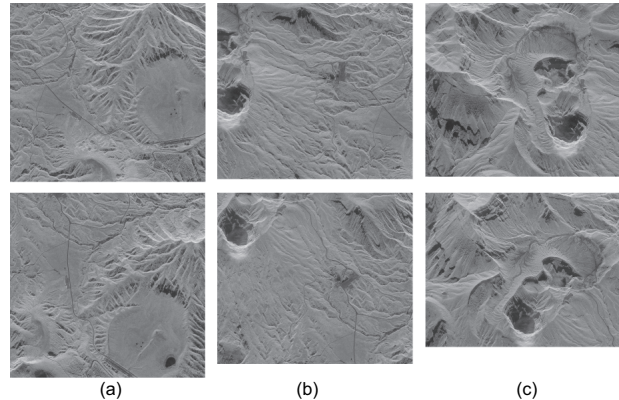


Fig. 3. Slant-range image pairs used in the experiments: (a) Aso A, (b) Aso B, and (c) Aso C.

images using the conventional method [9] and the proposed method. The measurement accuracy of each method is evaluated by comparing each result with a 5m-mesh digital elevation model (DEM) provided by the Geospatial Information Authority of Japan (GSI)¹. In the conventional method, the elevation values can be easily obtained from the measurement results since this method is based on a plane with 0m elevation. In the proposed method, the elevation values are obtained by converting the measurement results first into latitude, longitude, and ellipsoid height using the reference ellipsoid GRS80, and then converting them to elevation values using the geoid model of the Earth. The measurement accuracy of each method is evaluated by the mean and standard deviation of errors compared to the DEM. In the conventional method, the average height of the scene obtained from the metadata is used as the height of the ground projection plane before image correspondence. In the proposed method, the height of the ground projection plane is obtained by the procedure described in Sect. 2.4 (ii).

Fig. 4 shows the height maps and error maps for Aso A. Note that the gray color indicates the area where no corresponding points were obtained. No significant difference can be seen between both methods from the height maps. On the other hand, we can observe that the proposed method has less error in the whole scene from the error maps. Table 1 summarizes the mean and standard deviation of errors compared to the DEM for Aso A, B, and C. The proposed method without parameter optimization shows better performance than the conventional method by considering the Earth ellipsoid. The measurement accuracy of the conventional method is not improved by the parameter optimization, while that of the proposed method is improved by the parameter optimization.

4. CONCLUSION

We proposed a novel 3D measurement method from two SAR images using the principle of stereo vision. We used the Earth ellipsoid model in the SAR projection model, and considered a parameter optimization method without any prior knowledge of the scene. We demonstrated the effectiveness of the proposed method through experiments using airborne SAR images. In the future, we plan to further improve the correspondence matching step by considering the ground projection plane on a per pixel basis and we also plan

¹<https://www.gsi.go.jp/kiban/>

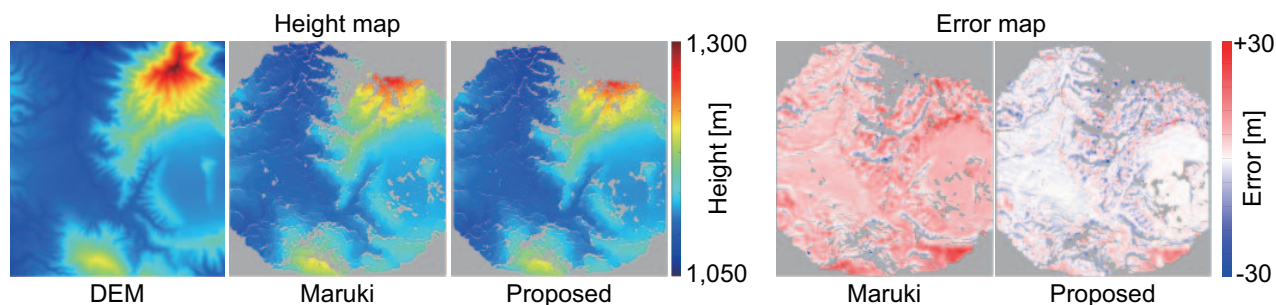


Fig. 4. Experimental results for Aso A.

Table 1. Mean and standard deviation of errors [m] compared to DEM.

Method	Parameter optimization	Aso A	Aso B	Aso C
Maruki [9]		-3.6 ± 3.2	-5.1 ± 3.3	-5.7 ± 4.0
	✓	6.1 ± 4.1	-1031 ± 200	-36.6 ± 9.7
Proposed		-1.9 ± 3.0	-4.1 ± 2.9	-5.3 ± 3.7
	✓	-0.4 ± 3.1	-1.7 ± 3.0	-2.5 ± 3.7

to evaluate our method using a Digital Surface Model (DSM) from scenes containing buildings and trees.

5. REFERENCES

- [1] J. A. Richards, *Remote Sensing with Imaging Radar*, Springer, 2009.
- [2] Norman Kerle, *Encyclopedia of Natural Hazards*, Springer Netherlands, 2013.
- [3] K. Omasa, F. Hosoi, and A. Konishi, “3D LiDAR imaging for detecting and understanding plant responses and canopy structure,” *J. Experimental Botany*, vol. 58, no. 4, pp. 881–898, 2007.
- [4] H. Guan, J. Li, Y. Yu, L. Zhong, and Z. Li, “DEM generation from LiDAR data in wooded mountain areas by cross-section-plane analysis,” *Int’l J. Remote Sensing*, vol. 88, no. 3, pp. 927–948, 2014.
- [5] J. Shan and A. Sampath, “Urban DEM generation from raw LiDAR data: A labeling algorithm and its performance,” *Photogrammetric Engineering & Remote Sensing*, vol. 71, no. 2, pp. 217–226, 2005.
- [6] A. Hirano, R. Welch, and H. Lang, “Mapping from ASTER stereo image data: DEM validation and accuracy assessment,” *ISPRS J. Photogrammetry and Remote Sensing*, vol. 57, no. 5, pp. 356–370, 2003.
- [7] P.A. Rosen, S. Hensley, I.R. Joughin, F.K. Li, S.N. Madsen, E. Rodriguez, and R.M. Goldstein, “Synthetic aperture radar interferometry,” *Proc. IEEE*, vol. 88, no. 3, pp. 333–382, Mar. 2000.
- [8] Henri Maître, *Processing of Synthetic Aperture Radar Images*, John Wiley & Sons, Ltd., 2010.
- [9] D. Maruki, S. Sakai, K. Ito, T. Aoki, J. Uemoto, and S. Uratsuka, “Stereo radargrammetry using airborne SAR images without GCP,” *Proc. IEEE Int’l Conf. Image Processing*, pp. 3585–3589, 2015.
- [10] K. Takita, M. A. Muquit, T. Aoki, and T. Higuchi, “A sub-pixel correspondence search technique for computer vision applications,” *IEICE Trans. Fundamentals*, vol. E87-A, no. 8, pp. 1913–1923, Aug. 2004.
- [11] S. Hishinuma, K. Ito, T. Aoki, J. Uemoto, and S. Uratsuka, “Elevation measurement from single-pass SAR images,” *Proc. IEEE Int’l Geoscience and Remote Sensing Symp.*, pp. 5662–5665, 2017.
- [12] K. Ito, S. Hishinuma, T. Aoki, J. Uemoto, and S. Uratsuka, “Towards on-board elevation measurement using interferometry and radargrammetry from single-pass SAR images,” *Proc. IEEE Int’l Geoscience and Remote Sensing Symp.*, pp. 5816–5819, 2018.
- [13] H. Imai, K. Ito, T. Aoki, J. Uemoto, and S. Uratsuka, “A method for observing seismic ground deformation from airborne SAR images,” *Proc. IEEE Int’l Geoscience and Remote Sensing Symp.*, pp. 1506–1509, 2019.
- [14] K. Ito, H. Imai, T. Aoki, and J. Uemoto, “Parameter optimization for detecting seismic ground deformation from airborne SAR images,” *Proc. IEEE Int’l Geoscience and Remote Sensing Symp.*, pp. 324–327, 2020.
- [15] K. Takita, T. Aoki, Y. Sasaki, T. Higuchi, and K. Kobayashi, “High-accuracy subpixel image registration based on phase-only correlation,” *IEICE Trans. Fundamentals*, vol. E86-A, no. 8, pp. 1925–1934, Aug. 2003.
- [16] M. A. Fisher and R. C. Bolles, “Random sample consensus: A paradigm for model fitting with applications to image analysis and automated cartography,” *Comm. ACM*, pp. 381–395, 1981.
- [17] A. Nadai, S. Uratsuka, T. Umehara, T. Matsuoka, T. Kobayashi, and M. Satake, “Development of X-band airborne polarimetric and interferometric SAR with sub-meter spatial resolution,” *Proc. IEEE Int’l Geoscience and Remote Sensing Symp.*, vol. 2, pp. II–913–II–916, July 2009.